Supplemental data.

Table S1. Primers employed for the generation of the *Pv*AMT1;1 mutants.

Mutant	Orientation	5'→ 3'
H211A	Sense	CTCCGCCGTTGTCGCTATGGTCGGCGGC
	Antisense	GCCGCCGACCATAGCGACAACGCCGGAG
H211E	Sense	CTCCGGCGTTGTCGAGATGGTCGGCGGCG
	Antisense	CGCCGCCGACCATCTCGACAACGCCGGAG
H377A	Sense	GCGGCGCAGCTGGCTGGAGGGTGCGG
	Antisense	CCGCACCCTCCAGCCAGCTGCGCCGC
H377E	Sense	GCGGCGCAGCTGGAGGGAGGGTGCGGC
	Antisense	GCCGCACCCTCCCTCCAGCTGCGCCGC
H125A	Sense	CGGCCTCACAGACATCGCCGCCCAGAATTTAGAC
	Antisense	GTCTAAATTCTGGGCGGCGATGTCTGTGAGGCCG
H125R	Sense	GGCCTCACAGACATCCGCGCCCAGAATTTAGAC
	Antisense	GTCTAAATTCTGGGCGCGGATGTCTGTGAGGCC

The underline bases are those that were changed to obtain the required mutation.

I) Calculation of the voltage dependence of PvAMT1;1 affinity (K_m) for ammonium (δ).

As shown in figure 2G of the main text, the affinity of *Pv*AMT1;1 for ammonium (K_m), was affected by voltage and pH, observing that at acidic pH (5.5) the affinity for ammonium showed a strong voltage dependence, decreasing at more positive membrane potentials; dependence that became smaller as the pH increased to pH 7.0, and becoming almost voltage independent at pH 8.0 (Fig. 2G, main text). Assuming a single binding site for ammonium, as indicated by the Michaelis-Menten kinetics, we made use of the method of Woodhull {Document not in library: (1)} (equation 1) to evaluate the voltage dependence of K_m,

$$K_m(\delta) = K_m^{(0\,mV)} * exp\,(\delta * e * \frac{V}{k*T}) \qquad (1)$$

where δ is the fractional electrical distance, *e* is the elementary charge, *V* is the membrane potential, *k* is Boltzmann's constant, and *T* is the absolute temperature {Document not in library: (1)}. Employing the program Origin 8.5 (OriginLab Co., MA, USA) we adjusted the results from figure 2G to an exponential ($r^2 = \geq 0.95$) to derive the value of δ from the slope that allowed us to determine that the location of the putative ammonium binding site within the membrane electrical field seems to move towards the extracellular side as the external pH is alkalinized, changing from (δ) 34% at pH 5.5 to 30% at pH 7.0 and to 21% at pH 8.0, a response that may be due to a screening effect caused by the higher concentration of protons associated with acidic pH.

II) Determination of the Stoichiometry of *Pv*AMT1;1

As demonstrated in figures 2C and 2D of the main text, the reversal potential showed sub-Nernstian responses to changes in both, extracellular ammonium and proton concentrations (pH) with slope values of 33 ± 3.7 and 26 ± 3.5 mV, respectively. According to our interpretation, the thermodynamic functioning of *PvAMT1;1* can be explained by equation (2) that defines the activity of a symporter (2), rather than by the Nernst equation.

$$E_r = \frac{1}{1+r}\,[E_H + rE_{NH_4^+}] \qquad (2)$$

where the stoichiometric ratio r = m/n and the Nernst potential for each ion, E_{H+} and E_{NH4+}, are given by equation 3 and 4, respectively:

$$n{NH_4}^+_o + m{H}^+_o \longleftrightarrow n{NH_4}^+_i + m{H}^+_i \qquad (3)$$

$$E_x = \frac{RT}{z_x F}\ln\left(\frac{[X]_o}{[X]_i}\right) \qquad (4)$$

where z_x is the ionic valance, R is the gas constant, T is temperature, F is Faraday's constant and [X] the ion activities out (o) or inside (i) the cell.

Applying equation (2) to data from figures 2C and 2E we calculated an *r* value of 0.8 ±.0.2 (n=6), that indicates *Pv*AMT1;1 functions as an H^+/NH_4^+ symporter with a 1:1 stoichiometry. This ratio value correlates with the intracellular acidification caused by the presence of ammonium, and the stimulation of the inward ammonium currents induced by low pH, and clearly supports the H^+/NH_4^+ symport mechanism for *Pv*AMT1;1.

1. Woodhull, a M. (1973) *The Journal of general physiology* **61**, 687-708
2. Accardi, A. and Miller, C. (2004) *Nature* **427**, 803-7

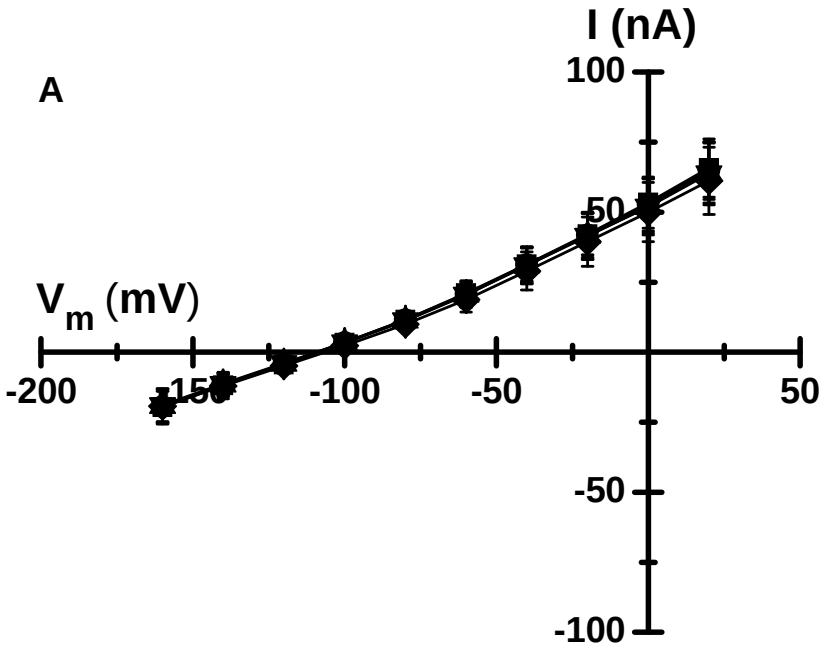

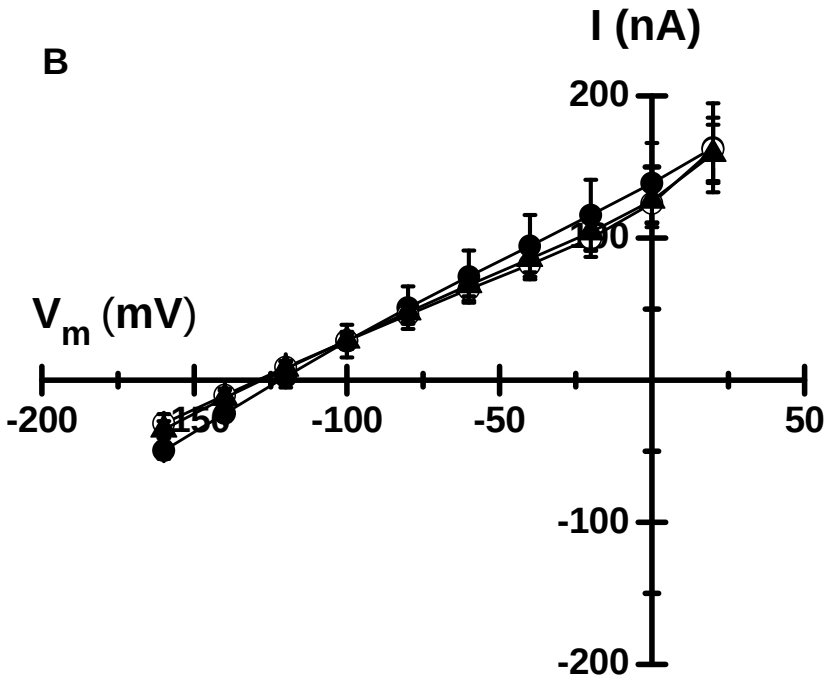

Supplentary Figure 1

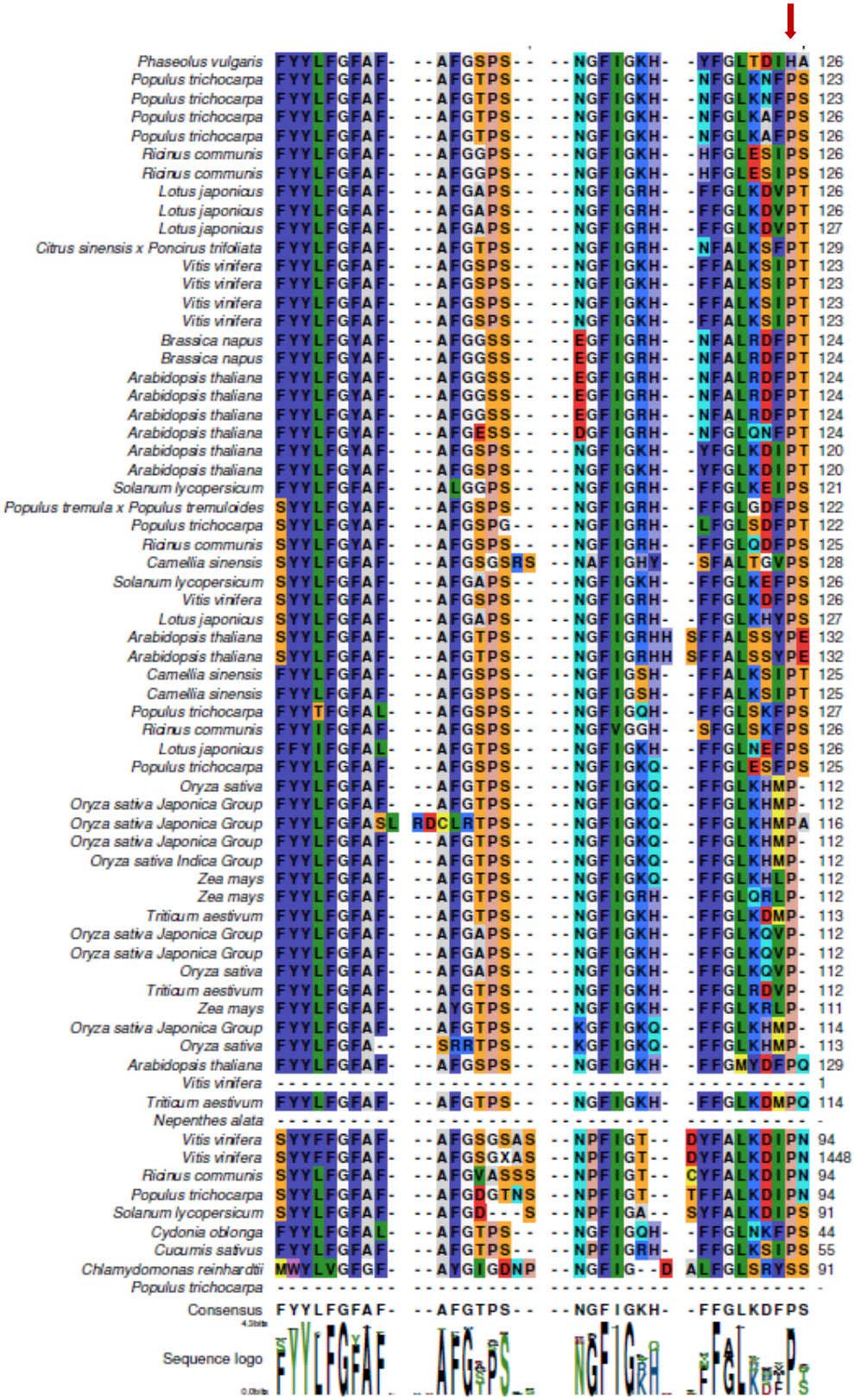

Supplementary Figure 2

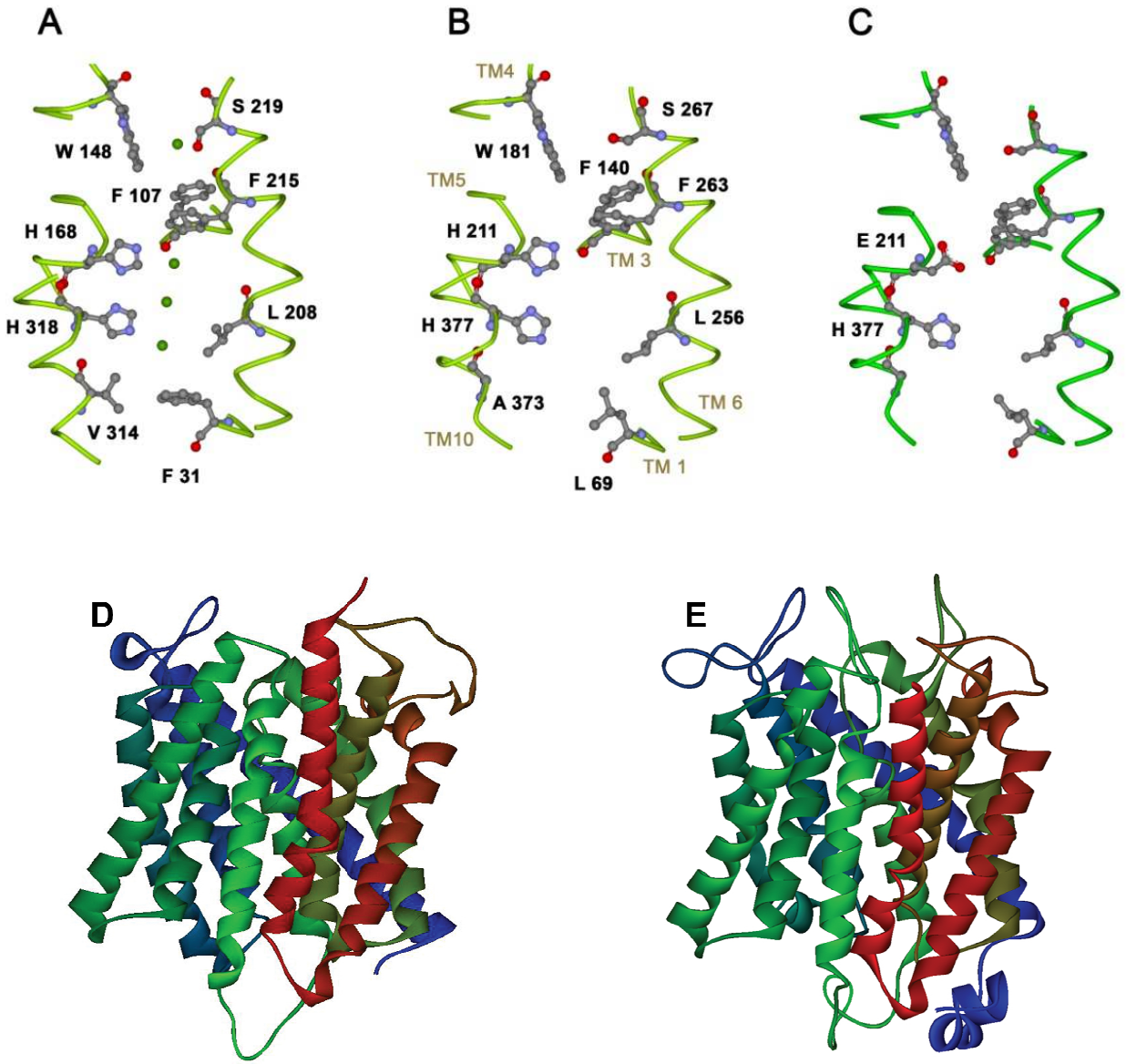

Supplementary Figure 3

Legends to Supplementary Figures

Supplementary Figure 1. Inward currents were not activated in water-injected oocytes by ammonium or in *PvAMT1;1*-injected oocytes in the absence of the cation at different pH. A Current-voltage (I-V) relationships showing that increasing ammonium concentrations (■ 10, ● 20, ▲80, ▼250 and ♦ 1000 µM) did not activate inward currents in water-injected oocytes. **B** Current-voltage relationships showing that **c**hanges in extracellular pH (● 5.5, ○ 7.0 and ▲8.0) had no effect on the currents recorded in the absence of ammonium in oocytes expressing *Pv*AMT1;1. Data represent the mean ± SD from more than 7 oocytes derived from more than three frogs.

Supplementary Figure 2. H125 is present exclusively in *Pv*AMT1;1 among the plant ammonium transporters. Sequence analysis of plant ammonium transporters showing the extracellular loop between transmembrane domains II and III. The arrow indicates the unique H125 in *Pv*AMT1;1; this residue is conserved among all the plant transporters and corresponds to Proline.

Supplementary Figure 3. Amino acids involved in ammonium transport in *Ec*AmtB are conserved in *Pv*AMT1;1., Pore region of *Ec*AmtB **(A)**, *Pv*AMT1;1 **(B)** and *Pv*AMT1;1H211E **(C)** showing that the amino acids proposed to be involved in ammonium transport in *Ec*AmtB are conserved and maintain similar positions in the common bean homologue *Pv*AMT1;1 and the mutant PvAMT1;1H211E. The green spheres in **(A)** represent NH_4^+/NH_3 molecules. Ribbon representation of the *Ec*AmtB **(D)** and *Pv*AMT1;1 **(E)** monomers, observe the longer extracellular loops in the latter. In all the figures the periplasmic/extracellular side is above.